Significance of Experimental Procedures on the Hot Corrosion Behavior of Nickel-Base Alloys under Cyclic Conditions

C. Leyens[1,*], I.G. Wright[2], B.A. Pint[2], and P.F. Tortorelli[2]

[1] DLR-German Aerospace Center, Institute of Materials Research, Cologne, Germany
[2] Oak Ridge National Laboratory, Corrosion Science and Technology Group, Oak Ridge, Tennessee, USA

Abstract

A simplified test procedure was established to assess the hot corrosion behavior of MCrAlY-type nickel-base alloys under the influence of molten sodium sulfate as well as sodium sulfate/potassium sulfate salt mixtures. Salt coated specimens were exposed to 1h thermal cycles at 950°C in flowing oxygen for up to 500 cycles. Mass change data of the specimens revealed a significant dependence of the corrosion attack not only, as expected, on the average contaminant flux rate, but also on the initial amount of salt deposited during each recoating cycle. Furthermore, deposit removal before salt recoating was found to markedly influence the corrosion attack of the alloys. This was related to changes in salt chemistry by the dissolution of elements such as Cr from the alloy which shifted the basicity of the salt and thus affected the extent of attack. Substituting Na for K in sodium sulfate/potassium sulfate salt mixtures generally resulted in a decreased attack. Although the high K-containing salts still caused significant attack typical of Type-I hot corrosion, the overall degration was much less than for sodium sulfate alone.

• At the time this work was performed the author was on sabbatical at Oak Ridge National Laboratory.

Introduction

Although new materials for high-temperature applications are mainly developed to provide high mechanical strength and creep resistance, it is mandatory to consider their hot corrosion behavior in the anticipated environment from the beginning of their development. Testing of the corrosion resistance of materials is also of great importance when well-established materials (or material systems including coatings) are to be operated in environments where the materials behavior is not well known. As the operating conditions for a specific material or material system can be quite complex, the optimum test would be to run the actual component in an existing facility or engine. However, as such a test is generally extremely costly, and as failure of the component may cause significant damage to the whole operating device, the component test is almost always the last step for a material to demonstrate its suitability for a specific application. Therefore, simplified corrosion tests are extremely desirable for research and development laboratories for use in developing an improved understanding of the corrosion mechanisms, as well as for industrial applications for cost-effective materials evaluation in a simulated environment. Unfortunately, no standardized test procedures have yet been established, and most research laboratories, materials manufacturers and also their customers have developed their own tests.

Recently, the European Federation of Corrosion has started an initiative to develop guidelines and standards for high-temperature corrosion research and testing [1]. Although simplified tests cannot (and are not intended to) simulate all aspects of actual operating conditions, standardized testing methods would be a great help in generating comparable data for materials evaluation. As for non-standardized tests, the question still to answer is related to how well the results of simplified tests correlate with the more complex service conditions of the “real world”. The degree of correlation will, in many cases, depend on the sophistication of the test and on the proper control of the relevant test parameters [2]. In some cases reasonable

correlation between laboratory tests and service experience has been achieved (for example, reference [3]).

Among laboratory tests, the discontinuous measurement of the high-temperature corrosive attack of materials is widely used (for example, references [4, 51). The most common methods are:

a) crucible tests, where the specimens are totally or partly immersed in a crucible containing a molten salt;
b) salt coat tests, where the specimens are coated with salt prior to exposure to high temperatures; and
c) burner rig tests, where the specimens are exposed to a burner into which flame contaminants can be injected.

Due to considerable differences in the test methods it is not surprising that the single results obtained from one of the above tests methods may differ significantly, and sometimes even do not reflect the same ranking for a variety of materials. However, even when one particular method is chosen, the results are strongly dependent on the exact testing procedure. The aim of the present paper was to assess the importance of test parameters in the salt test. Effects of salt deposit present on the specimen surface, the recoating frequency, removing the deposits before salt recoating, as well as the effect of the salt composition were investigated for the hot corrosion behavior of cast, model MCrAlY-type bond coat compositions under cyclic conditions. The specimens were tested in lh cycles at 950°C up to 500h and subsequently characterized by optical microscopy and scanning electron microscopy.

Experimental

The alloys included in this study included cast versions of NiCoCrAlY (Ni-22Co-18Cr-12.5Al-0.06Y, in wt.%) and NiCoCrAlYHfSi (Ni-20Co-18Cr-12.5Al-0.55Y-0.26Hf-0.37Si, in wt.%) coatings. The alloys were vacuum induction melted and cast in a water-chilled copper mold. The castings were then annealed at 1250°C for 4h in quartz ampules. Specimens (ø 1.5cm x 0.1-0.15cm) were cut from the castings and then polished with SiC paper to 600 grit, avoiding preferred orientation of the grinding marks. The 1h thermal cycles at 950°C were performed in an automated test rig in which the specimens were held in a vertical tube furnace by l't-Rh wire hooks for 1h and cooled to room temperature for 10min between cycles. Dry oxygen flowed continuously into the bottom of the tube during the exposures. SO, (of the order of 0.1 vol. percent) usually used in such tests was omitted to simplify operation. Since the hot corrosion scenario under consideration was that described by Bornstein [6] in which salt is delivered to the components by periodic shedding of compressor deposits, rather than by condensation of vapor species, this was considered a reasonable approach.

Prior to testing, all specimens were ultrasonically cleaned in acetone and methanol. For hot corrosion tests, the specimens were coated with water solutions of different salt compositions (Table I). The salt compositions were chosen to represent pure Na_2SO_4 (salt 1) which is widely used for hot corrosion studies, as well as to represent such deposits which are likely to form during combustion of biomass-derived fuels (salts 9 and 10) [7]. For the biomass-fuel related deposits, the higher K content was taken into account by three different K/Na ratios (K/Na=O, 2, and 15). The salt solutions were deposited onto the specimens using a dropper pipette, and the water was evaporated by heating the specimens on a hot plate up to about 200°C. In order to provide a uniform salt coating even at the beginning of the tests, the specimens were preoxidized for 1h at 950°C prior to coating, rather than depositing salt on the bare metal surface.

One set of NiCoCrAlY specimens was recoated with pure Na_2SO_4 after 20 and 100, 1 h cycle intervals ("recoating frequency"), respectively, applying different "contaminant flux rates" (CFRs) (Table II). In some cases the specimens were washed carefully in distilled water prior to recoating in order to remove the deposits. A second set of NiCoCrAlYHfSi specimens was coated with salts of different K/Na ratios (Table I) at an average CFR of $1.070 mg \cdot cm^{-2} \cdot h^{-1}$. These specimens were recoated every 100 cycles without deposit removal before recoating. All specimens were weighed before and after coating with salt and after washing, respectively, as well as before and after exposure, using a Mettler model AG245 analytical balance. Mass change of the specimens was calculated taking into account the continuous mass loss of the I't-Rh hooks. Corrosion products were characterized using optical microscopy (OM) and a field emission gun scanning electron microscope (FEG-SEM) equipped with energy dispersive x-ray analysis (EDXA).

Table I: K/Na and 2S/(Na+K) ratios for different salt compositions.

Designation	K/Na	2S/(Na+K)
salt 1	0	1
salt 9	2	1
salt 10	15	1

Table II: Amount of salt, recoating frequency, contaminant flux rate (CFR) and washing procedure of Na_2SO_4-coated cast NiCoCrAlY.

Designation	amount of salt [$mg \cdot cm^{-2}$]	recoating every	CFR [$mg \cdot cm^{-2} \cdot h^{-1}$]	washing before recoating
sample A	1.016±0.062	100h	$(1.016 \pm 0.062) \cdot 10^{-2}$	yes
sample B	1.061±0.072	100h	$(1.061 \pm 0.008) \cdot 10^{-2}$	no
sample C	0.262±0.050	20h	$(1.310 \pm 0.001) \cdot 10^{-2}$	yes
sample D	0.264±0.043	20h	$(1.320 \pm 0.002) \cdot 10^{-2}$	no
sample E	1.059±0.101	20h	$(5.295 \pm 0.005) \cdot 10^{-2}$	yes
sample F	1.051±0.156	20h	$(5.255 \pm 0.008) \cdot 10^{-2}$	no
sample G	*4.746t0.383*	20h	$(23.730 \pm 1.915) \cdot 10^{-2}$	yes
sample H	0.283±0.085	100h	$(0.283 \pm 0.001) \cdot 10^{-2}$	no

Results and Discussion

Effect of salt deposition procedure

An overview of the mass gain vs. number of 1h cycles data for Na_2SO_4-coated NiCoCrAlY specimens tested at 950°C is given in Fig. 1. The CFR was varied by almost two orders of magnitude between $0.283 \cdot 10^{-2}$ and $23.730 \cdot 10^{-2}$ $mg \cdot cm^{-2} \cdot h^{-1}$ and accordingly the extent of corrosive attack also differed widely. As expected, the highest mass loss was found for the highest CFR. Whereas at a first glance mass change data was in a scatter band for most specimens up to 350, 1h cycles, one specimen exposed to the highest CFR (sample G) and one specimen exposed to a fresh salt coating every 20h at an intermediate CFR (sample D) started to lose mass rapidly after 200-250, 1h cycles indicating an accelerated attack.

In Figs. 2-5 the mass change data for each specimen' are given in more detail. The open circles represent the overall specimen mass change after exposure including the deposits; whereas the filled circles represent mass change data obtained from the

specimens after salt removal and drying, thus excluding the mass of deposits. The mass change vs. time curves for a 100h recoating sequence revealed a strong depency of single data points on the washing procedure (Fig. 2). The data for sample A (washed, recoated every 100h, Fig. 2a) followed a zigzag course for the overall specimen mass change, which was characterized by mass gain after salt deposition and exposure, subsequent mass loss, and again mass gain. After 100 cycles no measurable amount of deposit was present on the specimen surface as indicated by specimen mass after washing; however, after 200,300, and 350 cycles, the specimen had lost mass after removing the deposits. As will be discussed in more detail later, the increasing mass loss with increasing numbers of cycles after washing was attributed to partial loss of the oxide scale during washing. Although the same CFR was applied to sample B (no washing, recoating every 100h) the mass change data were significantly different from that for sample A (Fig. 2b). Identical mass gain and mass loss behavior was found for samples A and B after 100 cycles, indicating good reproducibility of the testing procedures in general. However, after redepositing salt onto the already exposed surface of sample B the specimen gained mass continuously rather than discontinuously, as found for sample A. Furthermore, mass loss was evident from sample B after washing at the end of the test after ,350 cycles, whereas sample A exhibited a slight overall mass gain at the conclusion of the test. These results clearly indicate that, for the specific test parameters chosen in this study, deposit removal before salt recoating not only affected the mass gain data but also altered the extent of corrosion attack of the specimens.

Macrographs of both specimens revealed a considerable attack of the initially formed alumina scale (light gray phase) and the formation of spine1 phases (darker phases) on each of the specimen surfaces (Fig. 6A and B). The non-uniform attack of the alumina scale was attributed to local differences of the cast alloy chemistries which, in turn, affected the local scaling behavior. Furthermore, accelerated corrosion attack at the specimen edges was found, which was caused by salt accumulation at the edges relative to the flat specimen surfaces. Specimen edges also are susceptible to

corrosion since the increased. surface area leads to more rapid depletion of protective scale-forming elements, compared to the flat sides. It should be noted that salt accumulation at the edges (for the high CFRs) was not only a result of droplet formation during testing caused by gravitation, but was also caused by non-uniform wetting of the molten salt. Surface tension caused salt attraction to the edges over the entire circumference of the specimens, rather than only at the lowest point of the specimen suspended vertically in the tube furnace (see Fig. 6).

Mass change data was significantly affected by the initial amount of salt present on the surface, which depended for a given CFR on the recoating frequency, i.e. the number of cycles between salt redeposition cycles. Although the average CFRs were almost identical, mass change for sample C (washed, recoated every 20h) was apparently different from that of sample A (washed, recoated every 100h) (Figs. 2a and 3a). It should be noted that, due to the 5 times higher recoating frequency, sample C was coated with about 1/5 of the amount of salt compared to sample A on each recoating cycle. For samples A and C a similar mass gain peak at the beginning of the test was found, however, at longer times of exposure specimen C lost mass, and then started to gain mass again after about 220 cycles. Unlike the specimens recoated every 100 cycles, the overall specimen mass essentially mirrored the "real" specimen mass curve of sample C (including the mass of deposits). Even when the deposits were not removed from the surface before recoating (sample D, Fig. 3b) the shape of the mass change curve was almost identical to that obtained for the washed specimens. However, sample D gained mass after testing, whereas sample C lost mass. Comparison of Figs 2 and 3 led to the conclusions that 1) there was a significant effect on mass change not only of the average CFR but also of the actual amount of "fresh" salt present on the surface during exposure and that therefore 2) the recoating frequency considerably influenced the corrosion attack. The macrographs of the specimens after 350, lh cycles also revealed that the extent of attack was similar and independent of deposit removal before recoating when less salt was coated more frequently (Fig. 6, C and D). The amount of alumina scale

present on the surface of these specimens was much higher than for those specimens coated with a higher amount of salt at a lower recoating frequency (Fig. 6, A and B). Metallographic cross-sections are in preparation to verify the different extent of corrosion attack.

As expected, increasing the overall amount of salt on the specimen surfaces resulted generally in increased corrosion attack (Fig. 4). Coated with about 5 times the amount of salt of sample C, sample E lost mass continuously (Fig. 4a), again except for the first few cycles where slight mass gain was observed. The overall specimen mass mirrored the "real" specimen behavior but, of course, the specimen mass was always lower after washing due to loss of deposits and, especially after longer times of exposure, due to loss of parts of the oxide scale, as will be discussed later. In contrast to sample E where the deposits were removed before recoating every 20h, sample F (no washing before recoating every 20h) essentially gained mass with an increasing number of cycles (Fig. 4b). Even when the deposits were removed from sample F after the test, the "real" mass loss was not as great (about $7.5 mg \cdot cm^{-2}$) as that for sample E (about $40 mg \cdot cm^{-2}$). Therefore, Fig. 4 provides further evidence of the significance of deposit removal before recoating. Even though the amount of deposits present on the surface of sample F was steadily increased, the severity of the corrosion attack was less than for sample E which was confirmed by the macroscopic appearence of the specimens (Fig. 6, E and F), showing that sample E was much more degraded than sample F.

Comparison of mass data in Figs. 3 and 4 suggested a general trend of corrosion attack associated with deposit removal. For both the lower CFR applied to samples C and D (Fig. 3) and the higher CFR applied to samples E and F (Fig. 4) deposit accumulation apparently decreased the attack. Although the amount of salt was steadily increased on samples C and E the presence of the earlier deposit seemed to decrease the intensity of the attack. Based on the current understanding of the mechanisms of hot corrosion under salt deposits, fluxing of the alumina scale in the

presence of a molten salt is strongly dependent on the basicity of the salt [8]. Both basic and acidic fluxing are associated with a high and low oxide ion activity, respectively, and thus cause degradation of the alumina scale [9]. Although Cr_2O_3 is also soluble in fused Na_2SO_4 [10] Cr was reported to be effective in retarding accelerated attack of alumina scales. Goebel et al. [9] showed that for various Ni-base alloys Cr_2O_3 established an oxide ion activity in Na_2SO_4 that was not sufficient to maintain basic fluxing and is not low enough to cause acidic fluxing. Rapp et al. [11] subsequently showed that Cr_2O_3 dissolution buffers the oxide ion activity at a value near that at what Al_2O_3 has minimum solubility. Chromate fuel additives are known to effectively combat hot corrosion.

In the present study the yellow color of the deposits removed from the NiCoCrAlY specimens indicated the presence of sodium chromate (Na_2CrO_4), i.e. Cr was leached out of the substrates by the molten salt. In the case of salt deposition without deposit removal before recoating, the fresh salt was mixed with the salt that was already present on the surface for several cycles and that already contained a certain amount of Cr. With the addition of fresh salt the basicity of this salt was presumably less changed due to the presence of the "Cr buffer" compared to samples exposed to a fresh salt without any Cr-buffered deposit on the surface. In the latter case, the alumina scale was attacked more significantly.

The strongest attack of cast NiCoCrAlY was experienced with a CFR of $23.73 \cdot 10^{-2}$ $mg \cdot cm^{-2} \cdot h^{-1}$ (sample G, recoated every 20h, Fig. 5a). The specimen started losing considerable mass after about 200, lh cycles, and was heavily corroded after the test (Fig. 6, G). It should be noted that, for the chosen geometry of the specimens and their vertical suspension in the furnace, approximately 5 $mg \cdot cm^{-2}$ was the maximum amount of salt that could be coated without losing salt due to droplet formation and subsequent dripping during heating. In contrast to sample F, where a similar amount of salt deposit was accumulated after 5 recoating cycles, deposition of "fresh" salt every 20 h on sample G caused a very aggressive form of attack.

Again, the general shape of the overall mass change curve for sample G corresponded well with the "real" specimen mass data after deposit removal.

Surprisingly, the lowest CFR ($0.283 \cdot 10^{-2}$ mg·cm^{-2}·h^{-1}) applied in the tests to sample H did not result in a significantly lower mass change (Fig. 5b), although the specimen contained the highest amount of alumina on the surface after testing (Fig. 6, H). As for sample A, a zigzag mass change curve was obtained for sample H due to salt recoating after 100 cycles, which was somewhat in contrast to sample B (Fig. 2b) which continuously gained mass after the initial mass gain and mass loss sequence. Mass loss after washing of sample H at the end of the test revealed a slight salt accumulation during the test; however, it should be noted that some debris associated with some loss of oxide scale was found in the container after deposit removal.

Effect of salt evaporation

Comparison of the mass change data associated with recoating and deposit removal revealed that, for low amounts of salt coated onto the specimen, the mass loss by washing before recoating was fairly low (Fig. 7a). It should be noted that mass loss in general included not only salt deposits but also loss of oxide during washing which, however, was found to be marginal in the case of CFR=$1.310 \cdot 10^{-2}$mg·cm^{-2}·h^{-1}. For higher amounts of salt deposited on the surface (Fig. 7b) the absolute amount of salt present on the surface before washing was much higher indicating that the salt had not been completely evaporated within a period of 20, lh cycles. However, after about 200 overall cycles the mass loss after deposit removal started to increase. This unproportionally high mass loss of the specimen was associated with partial loss of the oxide scale in addition to the mass loss due to deposit removal during washing. The onset of an increasing amount of oxide loss during washing was correlated with the onset of accelerated specimen mass loss (compare Fig. 7b with Fig. 4a). As a result of rapid scale growth and continuing attack by fresh salt the mechanical integrity of the oxide scale was apparently significantly affected after longer times of exposure.

Once part of the oxide scale spalled, the next salt coating encountered either a thinner oxide scale or bare metal (depending on the type of spallation), thus further accelerating the attack.

A more detailed analysis of the evaporation behavior of the salt deposits is given in Fig. 8. The relative mass change of the specimens denotes the mass of the specimen during exposure in relation to its starting mass, including the fresh salt coating. It should be noted, of course, that the specimen mass was affected by superposition of mass gain as a result of corrosion and mass loss caused by salt evaporation and possibly oxide spallation. A more accurate determination of the salt evaporation rate would demand a very corrosion resistant alloy which forms a slow-growing well-adherent oxide scale. Due to the significant attack of the NiCoCrAlY alloy after extended exposure times associated with scale spallation, the evaporation rate was only calculated from a few data points. With this data the evaporation rate for pure sodium sulfate (salt 1) at 950°C in flowing oxygen was calculated to be roughly on the order of 0.01 $mg \cdot cm^{-2} \cdot h^{-1}$. However,, it should be noted that the salt evaporation rate was found to significantly depend on the alloy chemistry [9, 12] as the alloy composition in turn affected the deposit chemistry and, therefore, also its vapor pressure.

It was apparent from Fig. 8 that the sodium sulfate was evaporated from the NiCoCrAlY specimens at an almost linear rate, as observed for both $CFR=1.320 \cdot 10^{-2}$ $mg \cdot cm^{-2} \cdot h^{-1}$ and $CFR=5.255 \cdot 10^{-2}$ $mg \cdot cm^{-2} \cdot h^{-1}$. The data were determined at different times between different overall numbers of cycles. Deviation from linear behavior was observed at higher numbers of cycles and, to somewhat greater extent, for the higher CFRs. For higher numbers of cycles, side effects like oxide spallation and accelerated scale,re-growth during the 20 cycle periods accounted for the deviation from the linear behavior. For $CFR=5.255 \cdot 10^{-2}$ $mg \cdot cm^{-2} \cdot h^{-1}$, and more clearly for $CFR=23.730 \cdot 10^{-2}$ $mg \cdot cm^{-2} \cdot h^{-1}$ (not shown here), droplet formation and subsequent loss by dripping caused disproportionally high mass loss after the first few cycles (Fig. 8b)

but, once the "excess" salt was lost, again a linear evaporation rate was established (Fig. 8b, data points for 280-300h). It should be noted again that these data did not accurately reflect the salt evaporation behavior, because they included side effects related to oxide spallation. This was clearly indicated by the significant scatter of the data after 20 cycles, ranging from about zero to 40% relative mass change (Fig. 8).

Effect of salt composition

In order to assess the extent of corrosive attack likely to occur with the presence of contaminants typical of combustion products of biomass-derived fuels, NiCoCrAlYHfSi was exposed to different salt compositions representing K/Na ratios of 0, 2 , and 15. A stoichiometric sulfur content was established by using Na_2SO_4 and K_2SO_4 for preparation of the salt solutions. The average CFR was $1.0 \cdot 10^{-2} mg \cdot cm^{-2} \cdot h^{-1}$, and specimens were coated every 100h without deposit removal before recoating. The mass change vs. number of 1h cycles curves showed a significant effect of the K/Na ratio on the corrosion behavior. A decreased level of attack was associated with an increased K/Na ratio (Fig. 9). An alumina scale formed on all specimens in the initial stages of oxidation, However, degradation occurred after about 20 cycles for K/Na=O (pure Na_2SO_4) and after about 100, 1h cycles for K/Na=2 and 15. In the case of K/Na=O, the molten salt attack led to a rapid mass loss by oxide scale spallation, whereas K/Na=2 caused only moderate mass loss that started after recoating after 100, 1h cycles. Mass loss was caused by the formation of spine1 phases at the expense of protective alumina as a result of salt attack, and subsequent oxide spallation during thermal cycling. For K/Na=15, a mass gain was measured up to 500, 1h cycles, indicating reasonable adherence of the oxide scale.

After 500, lh cycles at 950°C, FEGSEM/EDS analysis of the specimen surfaces revealed spine1 phases as the main oxide phases (Fig. 10). Arrows in Fig. 10 indicate that the oxide scales spalled locally during cycling on all samples. The effect of (sulfate) salt composition can be summarized by the fact that the corrosion attack was significantly decreased with increasing K content in the molten salt. This effect

was found earlier also for a NiCoCrAlY alloy [13]. A more detailed study of the effect of the K/Na and 2S/(Na+K) ratio intended to simulate excess alkali conditions typical of some biomass fuels on the hot corrosion attack of NiCoCrAlYHfSi is discussed elsewhere [14].

Based on the present results, a 20h salt recoating frequency and an average contaminant flux rate on the order of $1.0 \cdot 10^{-2}$ $mg \cdot cm^{-2} \cdot h^{-1}$ with deposit removal before recoating was considered to provide the most consistent results regarding correlation between mass change data and actual corrosion attack of the specimens. However, the 20h salt recoating procedure was very labor-intensive. Therefore, for the sake of a reasonable specimen throughput (100, lh cycles per week) in the laboratory, the regular salt deposition procedure was chosen to be 1.0 $mg \cdot cm^{-2}$ salt recoated every 100h without deposit removal before recoating.

Summary and Conclusions

The hot corrosion behavior of NiCoCrAlY-type alloys under thermal cycling conditions was found to depend significantly on the testing procedures. The use of the contaminant flux rate alone as an average measure of the amount of deposits applied onto the specimens cannot be considered as a sufficient measure of the corrosion attack, when the contaminants are not applied continuously during exposure unlike in, for example, burner rig tests. For intermittent deposition of contaminants onto the specimens, a significant dependency of the corrosion attack on the recoating frequency was evident. Even when the same average contaminant flux rate was applied, mass change data revealed that the corrosion attack was less severe for those specimens coated more frequently but with a lower amount of salt on each recoating step. Therefore, it is suggested that for hot corrosion tests with intermittent salt deposition, the “recoating frequency” must be always considered along with the average “contaminant flux rate”. Furthermore, the effect of deposit removal should be taken into account when data from different corrosion tests are

compared. However, the effect of recoating frequency is minor compared to that of the contaminant flux rate and deposit removal or retention. Deposit removal (washing) before recoating may result in an accelerated attack, due to a change of the basicity of the molten salt compared to deposits which where present on the surface for longer exposure times.

Whenever material behavior is to be assessed by simplified corrosion tests it is necessary to simulate the anticipated environment as closely as possible. For different K/Na ratios which were considered to be relevant to combustion product obtained from biomass-derived fuels, a significantly different corrosion attack was observed, showing that seemingly minor changes in the deposit chemistry may cause a different extent of corrosion attack.

Acknowledgments

Research sponso[illegible]y the U.S. Department of Energy, Assistant Secretary for Energy Efficiency and [illegible]vable Energy, Office of Industrial Technologies, as part of the Advanced Turb[illegible] Systems Program under contract DE-AC05-96OR22464 with Lockheed Marti[illegible]ergy Research Corporation, and the German Aerospace Center. M. I'. Brady, D.i[illegible]'ilson, and J.R. DiStefano at ORNL provided comments on the manuscript.

References

[1] H.J. Grabke and D.B. Meadowcroft, Guidelines for Methods of Testing and Research in High Temperature Corrosion, (The Institute of Materials, London, 1995)
[2] I'. Hancock, Corrosion Science, 22(1)(1982), 51-65.
[3] S.R.J. Saunders, Materials Science and Technology, 2(1986), 282-289.
[4] P. Steinmetz, C. Duret, and R. Morbioli, Materials Science and Technology, 2(1986), 262-271.

[5] J.R. Nicholls, in: Guidelines for Methods of Testing and Research in High Temperature Corrosion, ed. H.J. Grabke and D.B. Meadowcroft (London: The Institute of Materials, 1995), 11-36.
[6] N.S. Bornstein and W.P. Allen, Materials Science Forum, 251-254(1997), 127-134.
[7] I.G. Wright, C. Leyens, and B.A. Pint, unpublished research, 1999
[8] R.A. Rapp and Y.S. Zhang, JOM, (12)(1994), 47-55.
[9] J.A. Goebel, F.S. Pettit, and G.W. Goward, Metallurgical Transactions, 4(1973), 261-278.
[10] Y.S. Zhang, Journal of the Electrochemical Society, 133(1986), 655-657.
[11] R.A. Rapp, Materials Science and Engineering, 87(1987), 319-327.
[12] C. Leyens, unpublished research, 1999
[13] C. Leyens, I.G. Wright, and B.A. Pint, in: Elevated Temperature Coatings: Science and Technology III, ed. J. Hampikian and N.B. Dahotre (Warrendale: The Minerals, Metals and Materials Society, 1999), 79-90
[14] C. Leyens, LG. Wright, B.A. Pint, and P.F. Tortorelli, unpublished research, 1999

List of Figures

Figure 1: Mass change vs. number of 1h cycles curves for Na_2SO_4-coated NiCoCrAlY (overview, for details refer to Figs. 2-5). Specimens were coated with different CFRs at different time intervals. Some specimens were washed to remove salt deposits before recoating with salt. Specimen designation is according to Table II.

Figure 2: Mass gain vs. number of 1h cycles curves for Na_2SO_4-coated NiCoCrAlY. The CFR was $1.016 \cdot 10^{-2}$ $mg \cdot cm^{-2} \cdot h^{-1}$ (a) and $1.061 \cdot 10^{-2}$ $mg \cdot cm^{-2} \cdot h^{-1}$ (b), respectively. Both specimens were recoated every 100h and deposits were removed before recoating on *Sample A*. *Sample B* was only washed at the end of the test.

Figure 3: Mass gain vs. number of 1h cycles curves for Na_2SO_4-coated NiCoCrAlY. The CFR was $1.310 \cdot 10^{-2}$ $mg \cdot cm^{-2} \cdot h^{-1}$ (a) and $1.320 \cdot 10^{-2}$ $mg \cdot cm^{-2} \cdot h^{-1}$ (b), respectively. Both specimens were recoated every 20h and deposits were removed before recoating on *Sample* C. *Sample D* was only washed at the end of the test. Note that the ordinates have different scales.

Figure 4: Mass gain vs. number of 1h cycles curves for Na_2SO_4-coated NiCoCrAlY. The CFR was $5.295 \cdot 10^{-2}$ $mg \cdot cm^{-2} \cdot h^{-1}$ (a) and $5.255 \cdot 10^{-2}$ $mg \cdot cm^{-2} \cdot h^{-1}$ (b), respectively. Both specimens were recoated every 20h and deposits were removed before recoating on *Sample E*. *Sample F* was only washed at the end of the test. Note that the ordinates have different scales.

Figure 5: Mass gain vs. number of 1h cycles curves for Na_2SO_4-coated NiCoCrAlY. The CFR was $23.730 \cdot 10^{-2}$ $mg \cdot cm^{-2} \cdot h^{-1}$ (a) and $0.283 \cdot 10^{-2}$ $mg \cdot cm^{-2} \cdot h^{-1}$ (b), respectively. *Sample* G was recoated every 20h and deposits were removed before recoating. *Sample H* was recoated every 100h and only washed at the end of the test. Note that the ordinates have different scales.

Figure 6: Macroscopic images of Na_2SO_4-coated NiCoCrAlY specimens after 350, 1h cycles. Light gray oxide scales represent alumina whereas darker parts of the specimens surfaces mainly consist of spine1 phases. Letters designating the specimens correspond to Table II. Note that the initial diameter of the specimens was 15mm.

Figure 7: Relative mass change vs. number of lh cycles for two NiCoCrAlY specimens Na_2SO_4-coated at different CFRs. Different sets of data points were taken after different numbers of cycles. E.g., between 280 and 300

cycles data was recorded after 281, 283, 285, 290, 295, and 300h. Mass loss of the specimens is partly a result of salt evaporation during exposure (refer to text for details).

Figure 8: Mass change vs. number of lh cycles for two NiCoCrAlY specimens Na_2SO_4-coated at different CFRs. Mass gain is attributed to the amount of salt added whereas mass loss is mainly due to salt evaporation and loss of oxide scale during cleaning (refer to text for details).

Figure 9: Mass change vs. number of 1h cycles for NiCoCrAlHfSi alloy salt coated with three different K/Na ratios and 2S/(Na+K)=1 the latter representing a stoichiometric S content. The average CFR was 1.070 $mg \cdot cm^{-2} \cdot h^{-1}$. Mass loss for K/Na=O was as high as 5.8 $mg \cdot cm^{-2}$ after 500, 1h cycles.

Figure 10: SEM micrographs of NiCoCrAlYHfSi specimens after 500, 1h cycles. a) K/Na=O, b) K/Na=2, c) K/Na=15. Arrows indicate surface areas where parts of the oxide scale spalled during exposure at 950°C or on cooling down to room temperature between the cycles. Note that spine1 phases were the main oxide phases present on the surfaces on all specimens.

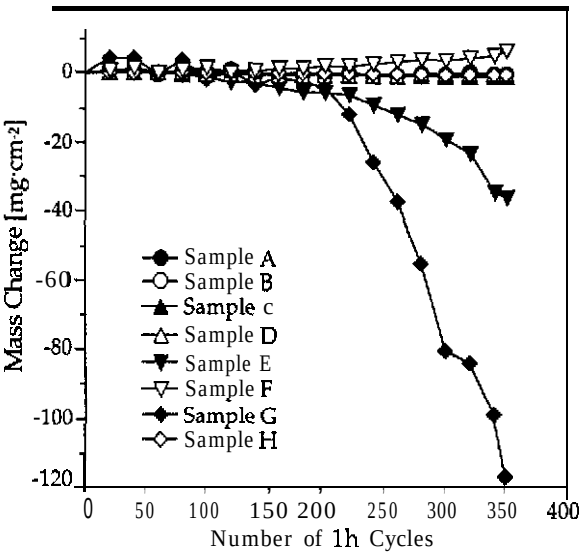

Figure 1

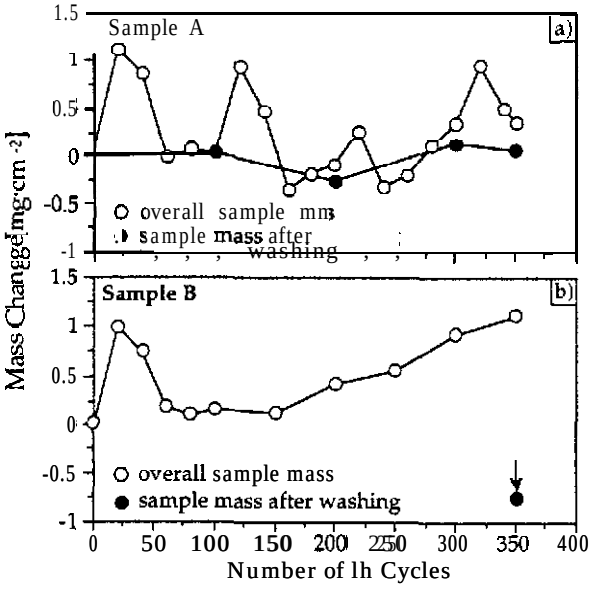

Figure 2

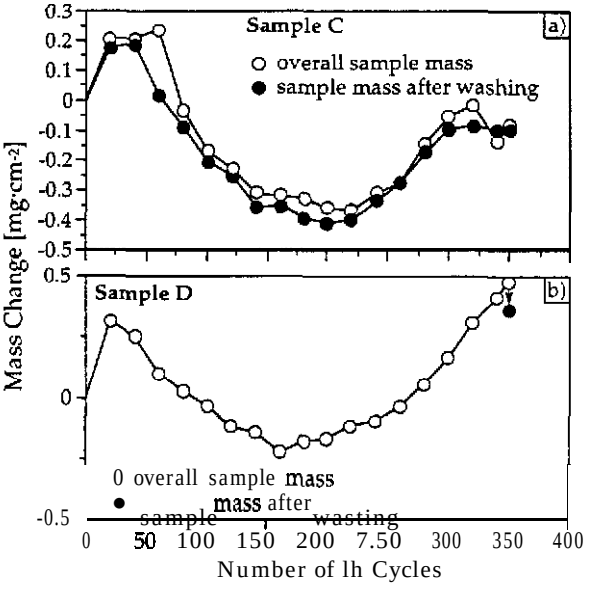

Figure 3

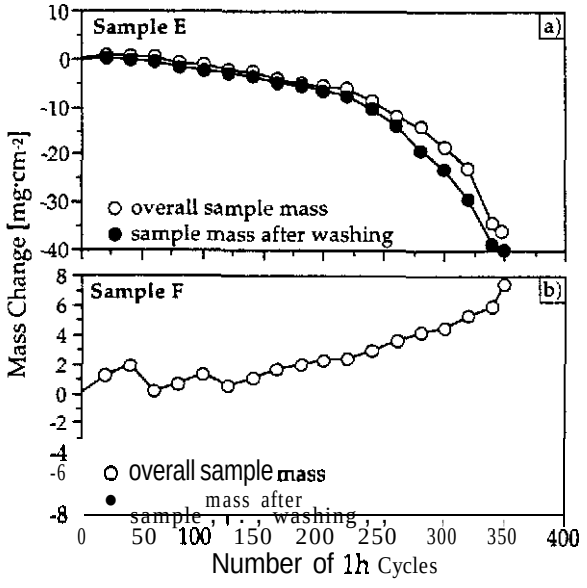

Figure 4

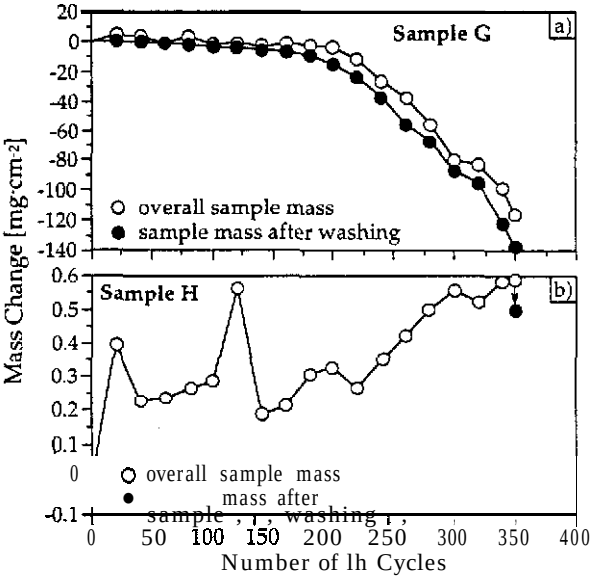

Figure 5

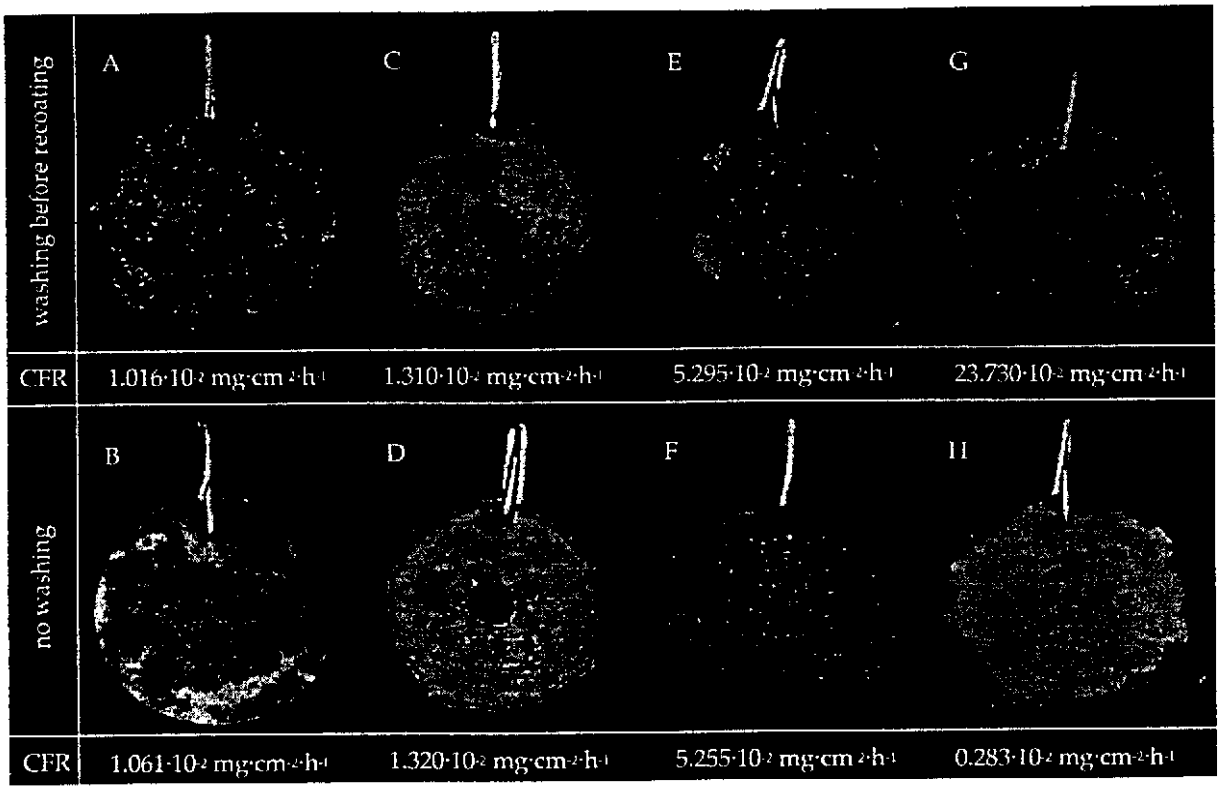

Figure 6

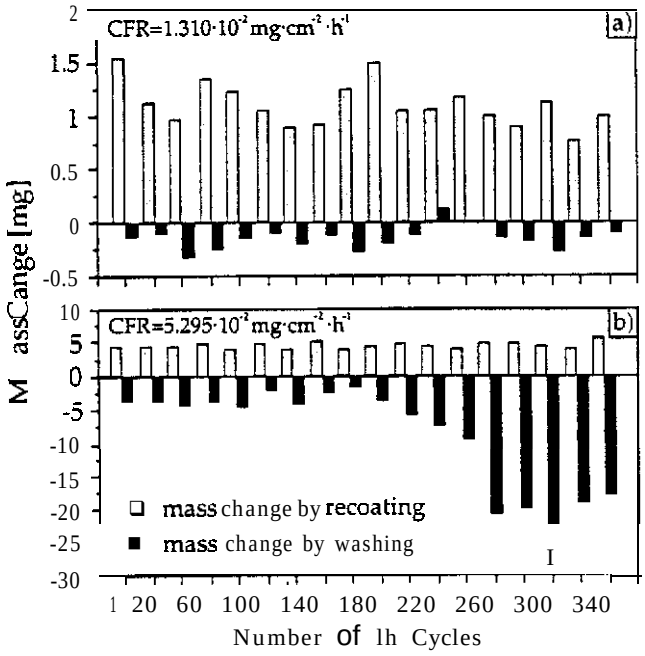

Figure 7

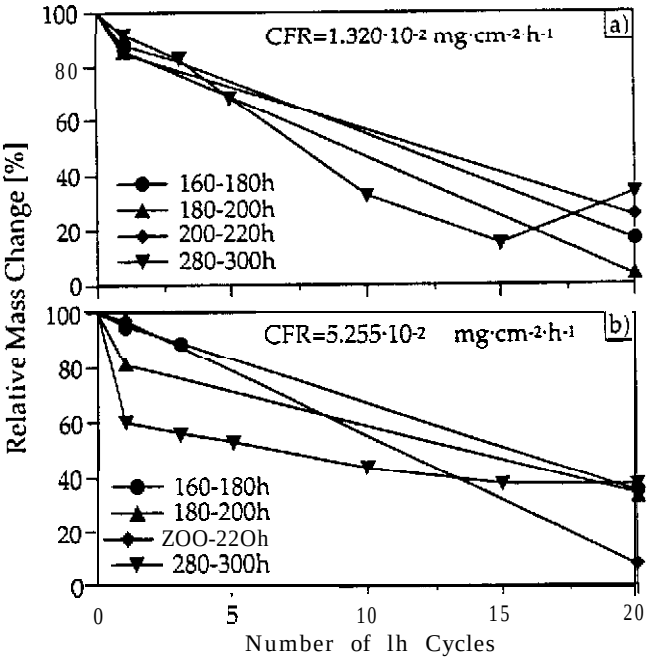

Figure 8

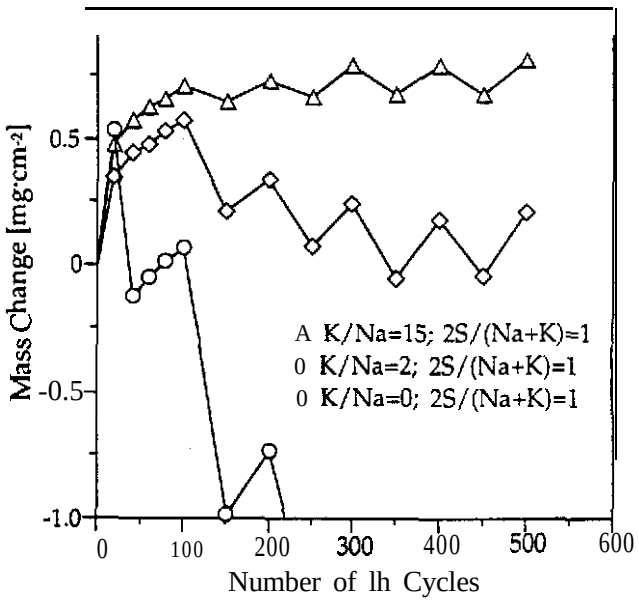

Figure 9

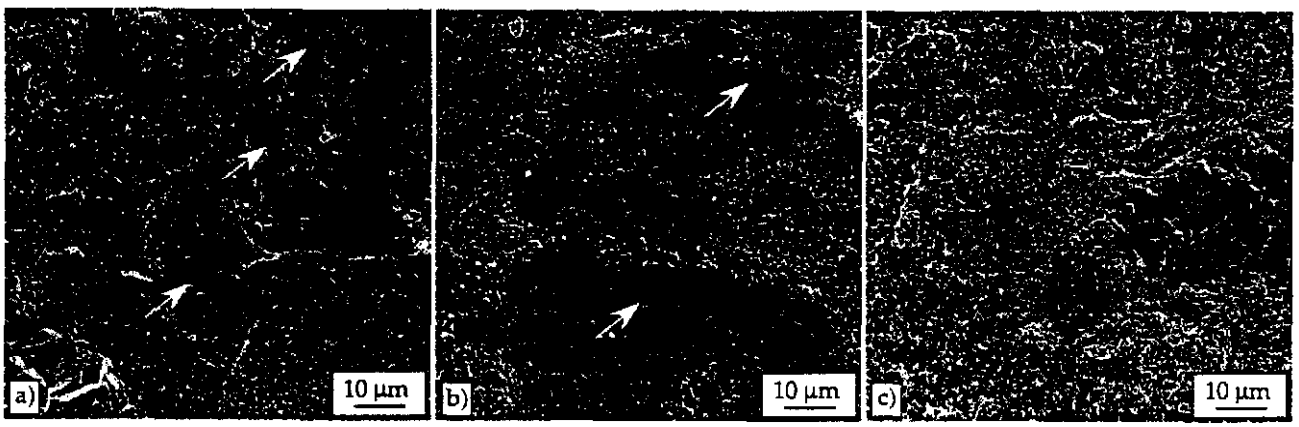

Figure 10